

Test of prototype ITER vacuum ultraviolet spectrometer and its application to impurity study in KSTAR plasma

C. R. Seon, J. H. Hong, J. Jang, S. H. Lee, W. Choe, H. H. Lee, M. S. Cheon, S. Pak, H. G. Lee, W. Biel, and R. Barnsley

Citation: *Review of Scientific Instruments* **85**, 11E403 (2014); doi: 10.1063/1.4886430

View online: <http://dx.doi.org/10.1063/1.4886430>

View Table of Contents: <http://scitation.aip.org/content/aip/journal/rsi/85/11?ver=pdfcov>

Published by the AIP Publishing

Articles you may be interested in

Edge impurity rotation profile measurement by using high-resolution ultraviolet/visible spectrometer on J-TEXTa)
Rev. Sci. Instrum. **85**, 11E423 (2014); 10.1063/1.4891927

First measurements of highly ionized impurity emission distribution by grazing-incidence flat-field extreme ultraviolet spectrometer in HL-2Aa)
Rev. Sci. Instrum. **85**, 11E426 (2014); 10.1063/1.4891708

Space-resolved vacuum ultraviolet spectrometer system for edge impurity and temperature profile measurement in HL-2A
Rev. Sci. Instrum. **81**, 043503 (2010); 10.1063/1.3378288

High efficiency extreme ultraviolet overview spectrometer: Construction and laboratory testing
Rev. Sci. Instrum. **77**, 10F305 (2006); 10.1063/1.2221659

Radial profile measurement of impurity line emissions using space-resolved 3 m vacuum ultraviolet spectrometer in LHD
Rev. Sci. Instrum. **77**, 10F307 (2006); 10.1063/1.2221594

The new SR865 *2 MHz Lock-In Amplifier* ... \$7950



SR865 2 MHz Lock-In Amplifier

Features:

- Intuitive front-panel operation
- Touchscreen data display
- Save data & screen shots to USB flash drive
- Embedded web server and iOS app
- Synch multiple SR865s via 10 MHz timebase I/O
- View results on a TV or monitor (HDMI output)

Specs:

- 1 mHz to 2 MHz
- 2.5 nV/√Hz input noise
- 1 μs to 30 ks time constants
- 1.25 MHz data streaming rate
- Sine out with DC offset
- GPIB, RS-232, Ethernet & USB

Stanford Research Systems
www.thinkSRS.com • Tel: (408)744-9040

Test of prototype ITER vacuum ultraviolet spectrometer and its application to impurity study in KSTAR plasmas^{a)}

C. R. Seon,^{1,b)} J. H. Hong,² J. Jang,² S. H. Lee,² W. Choe,² H. H. Lee,¹ M. S. Cheon,¹ S. Pak,¹ H. G. Lee,¹ W. Biel,³ and R. Barnsley⁴

¹National Fusion Research Institute, Gwahangno 113, Yuseong-gu, Daejeon, South Korea

²Korea Advanced Institute of Science and Technology, Gwahangno 335, Yuseong-gu, Daejeon, South Korea

³Institut für Plasmaphysik, Forschungszentrum Jülich GmbH, EURATOM Association, Trilateral Euregio Cluster, D-52425 Jülich, Germany

⁴ITER Organization, Cadarache Centre, 13108 Saint-Paul-Lez-Durance, France

(Presented 4 June 2014; received 31 May 2014; accepted 19 June 2014; published online 10 July 2014)

To optimize the design of ITER vacuum ultraviolet (VUV) spectrometer, a prototype VUV spectrometer was developed. The sensitivity calibration curve of the spectrometer was calculated from the mirror reflectivity, the grating efficiency, and the detector efficiency. The calibration curve was consistent with the calibration points derived in the experiment using the calibrated hollow cathode lamp. For the application of the prototype ITER VUV spectrometer, the prototype spectrometer was installed at KSTAR, and various impurity emission lines could be measured. By analyzing about 100 shots, strong positive correlation between the O VI and the C IV emission intensities could be found.

© 2014 AIP Publishing LLC. [<http://dx.doi.org/10.1063/1.4886430>]

I. INTRODUCTION

Monitoring of impurity contents has the significance related to the plasma performance and the lifetime issue of plasma facing components in the ITER tokamak.^{1–3} The role of ITER vacuum ultraviolet (VUV) core survey spectrometer is to measure VUV emission lines and to identify all relevant impurity species in the ITER main plasmas. It is one of three ITER VUV subsystems that monitor impurities with full coverage in core, edge, and divertor plasmas.

The ITER VUV core survey spectrometer has to be designed so that high spectral resolution ($\lambda/\Delta\lambda$) of 200–500 is attained in the wide wavelength range of 2.4–160 nm. To achieve this aim, the VUV core survey spectrometer was designed as a five-channel spectral system.^{3–5} To investigate the optimal design of multi-channel spectrometer, a two-channel prototype spectrometer has been developed with No. 3 (14.4–31.8 nm) and No. 4 (29.0–60.0 nm) among 5 channels (2.4–160 nm).⁴

To confirm the optical system and also to analyze the measured line intensities, the intensity calibration of the spectrometer is required. For this reason, the absolute intensity calibration was performed in the laboratory using emission lines from the hollow cathode lamp, which is an absolutely calibrated source by comparing with the incident photon number from the electron storage ring BESSY in Berlin.^{6,7}

For application of the calibrated prototype ITER VUV spectrometer, it was installed at KSTAR, and impurity lines were measured for two campaign periods (2012–2013). From the measured spectra and the calibration curve, the line

integrated emission intensity of various impurity species was derived. By analyzing about 100 shots, correlations between various impurity lines and plasma parameters were derived, and a strong correlation between different impurity species such as C IV, O VI was found.

II. EXPERIMENTAL SETUP

The ITER prototype system consists of a toroidal mirror, two holographic diffraction gratings with toroidal geometry, and two different electronic detectors, as shown in Fig. 1(a).⁴ A common slit with 10 mm × 114 μm size is positioned in the slit chamber. Two kinds of detectors of the micro-channel plate (MCP) electron multiplier with camera (McPherson Co.) and the back-illuminated charge coupled device (Princeton Instruments Co.) are installed at Ch. 3 and Ch. 4, respectively. It is noted that the quantum efficiency of micro channel plate (MCP) is 15%–20% for VUV light,⁸ and the back-illuminated CCD (BI-CCD, Princeton Instruments Co.) quantum efficiency is 41%–45% at 10–100 nm wavelength.^{9,10}

The calibrated hollow cathode lamp was used as a light source with current 1–2 A and DC voltage 400–500 V. The Ne and He gases were used because various intensive lines of Ne II, He II, and He I exist in the wavelength range 15–60 nm. The distances from the light source to the collimating mirror and from the collimating mirror to the slit are 650 mm and 450 mm, respectively. In the calibration experiment, two 114 μm × 3 mm slit regions (3 mm up and 3 mm down from the slit center) were used for each channel.

For collimation of the VUV light to the slit, a gold coated toroidal mirror with 75° incidence angle was adopted. The toroidal mirror size is 72 mm (width) × 46 mm (height), and the mirror surface roughness is 0.5 nm (rms). The radius

^{a)}Contributed paper, published as part of the Proceedings of the 20th Topical Conference on High-Temperature Plasma Diagnostics, Atlanta, Georgia, USA, June 2014.

^{b)}Author to whom correspondence should be addressed. Electronic mail: crseon@nfri.re.kr.

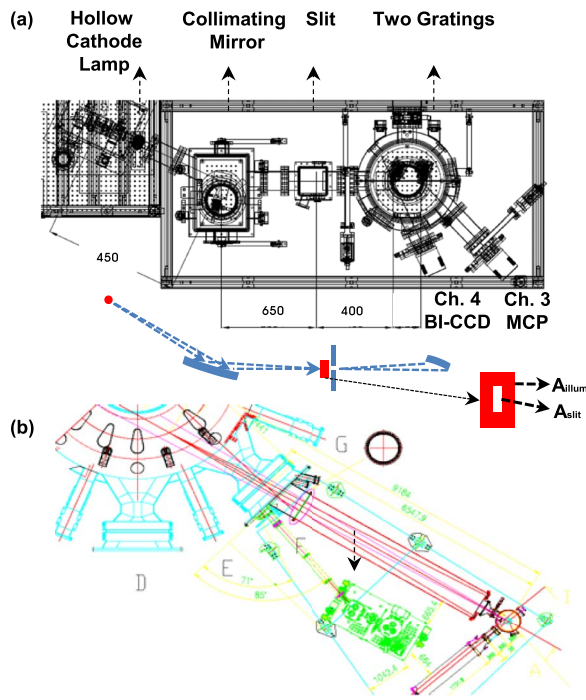


FIG. 1. (a) The VUV spectrometer prototype system. A collimation mirror, two gratings, and two different detectors were installed. The illuminated area (red rectangle) of the light source (circle) is larger than the slit area. (b) The VUV spectrometer prototype system at KSTAR. Measurement of line integrated VUV light without spatial resolution.

of curvature is 2370 mm (width) and 500 mm (height), respectively.

III. INTENSITY CALIBRATION

The calibrated hollow cathode lamp was used for the intensity calibration of the spectrometer. The photon number incident on the slit of the emission line was divided by the measured detector counts and the spectrometer etendue. The inverse sensitivity of the spectrometer, p^{-1} [photons/(counts mm² sr)] is given as

$$p^{-1} = P/(S \cdot \text{etendue}) \quad (1)$$

where P [photons/s] is the photon number per a second incident on the slit, S [counts/s] is the signal count rate for each emission line on the detector, and etendue [mm² sr] is the multiplication of the solid angle of the grating [sr] and the slit area [mm²].

To derive the incident photon number P [photons/s], the known values of emission power per solid angle, I [W/sr] from Table I of Ref. 11 are used for each emission line of the hollow cathode lamp. However, it is difficult to use I values directly to obtain P values in this experimental setup. As shown in Fig. 1(a), the imaging area of the light source (1.2 mm diameter) on the slit is larger than the slit size (114 $\mu\text{m} \times 3$ mm) of each spectrometer, because the collimation mirror geometry is designed to use a common long slit 10 mm (vertically not focused). For this reason, the incident photon number P is expressed as

$$P = I/(hc/\lambda) \cdot \Omega \cdot R \cdot (A_{\text{slit}}/A_{\text{illum}}), \quad (2)$$

where hc/λ , Ω , R , and $A_{\text{slit}}/A_{\text{illum}}$ is the photon energy [J], the solid angle of the light source on the effective mirror area [sr], the mirror reflectivity, and the ratio of the slit area [mm²] to the illuminated area [mm²] of the light source, respectively. The effective mirror area is determined from the grating size and the grating diverging angle for each channel, as shown in Fig. 1(a). The effective mirror area is 16 mm (height) \times 28 mm (width) for channel 3 and 12 mm \times 34 mm for channel 4.

The illuminated area of the light source, A_{illum} on the slit position was calculated using the ray-tracing tool, ZEMAX. The image of 1.2 mm diameter source on the slit is $A_{\text{illum}} = 17.5$ mm (height) \times 2.0 mm (width) for channel 3, and 19.5 mm (height) \times 1.8 mm (width) for channel 4. By comparison of the illuminated area with the slit area A_{slit} , the incident photon number on the slit, P could be obtained using Eq. (2) for each channel.

From calculating Eq. (2) with reference emission power I of He I A, Ne I A discharge,¹¹ the incident photon number, P was derived for emission lines of Ch. 4 range (29–60 nm). The detector counts S of the back-illuminated CCD Ch. 4 was measured for each emission line. From Eq. (1), the inverse sensitivity p^{-1} of the Ch. 4 spectrometer could be found as shown in 30 nm – 60 nm region of Fig. 2. The error of the calibration points is about 30% (the back-illuminated CCD detector counts 15%, the ray tracing error 15%, the hollow cathode lamp discharge condition instability 15%). The expected sensitivities (solid curve of Fig. 2) could be obtained by multiplying the detector efficiency 0.35–0.43 and the grating efficiency 0.75–0.11 depending on the wavelength.

To calibrate channel 3 spectrometer with MCP + camera detector, it is necessary to find the detector efficiency. To derive the detector efficiency of MCP + camera, the cross calibration between Ch. 3 (MCP) and Ch. 4 (back-illuminated CCD) was performed by using the common spectral line of He II 30.4 nm. From comparing the detector counts at Ch. 3 and Ch. 4 for the common line He II 30.4 nm, the MCP detector efficiency was found to be 16% of the back-illuminated CCD efficiency in this experiment setup. As the back-illuminated CCD detector efficiency is 41% at 30.4 nm, the total system of MCP + camera shows the efficiency of 8%. From the reference values,⁸ the MCP quantum efficiency is about 22%–28% depending on the wavelength. Consequently, it is deduced that the detector efficiency of MCP + camera

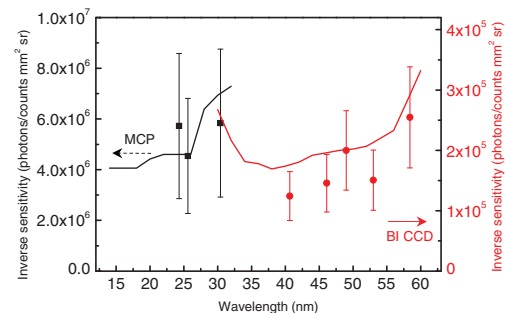


FIG. 2. Inverse sensitivities, p^{-1} of the spectrometers. Dots are calibration points obtained experimentally using the hollow cathode lamp and curves are calculated from efficiencies of optical components. Left y-axis is the inverse sensitivity of Ch. 3 using MCP detector (black) and right y-axis is the inverse sensitivity of Ch. 4 using back-illuminated CCD detector (red).

setup is 6%–8% in the wavelength range of 15–30 nm. The measured sensitivity values for Ch. 3 are plotted in Fig. 2, where the solid curve is the sensitivity from the grating and the detector efficiency. The error of the calibration point is about 50% (detector efficiency from cross calibration 30%, detector counts 15%, ray tracing error 15%, hollow cathode lamp discharge condition stability 15%). Finally, it was found that the measured detector counts were in accordance with the expected counts in the overall wavelength range 15–60 nm. The main reason of the discrepancy is that the pressure dependence of the hollow cathode lamp was larger than expected and it was difficult to maintain the pressure to be the same as the reference values.

IV. APPLICATION TO KSTAR PLASMAS

To verify the prototype ITER VUV spectrometer in tokamak environment, the two-channel spectrometer was installed at KSTAR. For application of the prototype VUV spectrometer to KSTAR, a different collimation mirror set was implemented to collimate light from the plasma in the long distance, ~ 6 m. The mirror reflectivity of this mirror set with surface roughness 4 nm and incidence angle 75° could be derived from the calculation.

From the calculated mirror reflectivity, the grating efficiency and the detector efficiency, a different calibration curve was derived for KSTAR experiment.

As shown in Fig. 1(b), two-channel VUV spectrometer was installed at KSTAR, so that various impurity species could be identified from KSTAR plasmas. From various shots, the typical impurity emission lines of Fe XVI, Fe XV, He II, C IV, Ar XV, Ar XVI, and O VI could be identified, as shown in Fig. 3. The line integrated emission intensity was derived from the calibration curve and the emission intensity of Ar XVI (35.4 nm) line was about 0.2×10^{13} – 5×10^{13} photons/mm² s for typical shots. In Fig. 3, the spectra of 29–60 nm with back-illuminated detector shows better resolution than the spectra of 15–31 nm with MCP detector due to smaller pixel size of the back-illuminated CCD.⁴

From data in two campaign periods (2012–2013), statistical analysis was performed for various impurity lines and plasma parameters. Impurity line intensity and plasma parameters at the flat top region were chosen. From analysis, a strong positive correlation between C IV (38.4 nm) and O VI (17.3 nm) emission intensity was found as shown in Fig. 4. In Fig. 4, intensities are normalized by line integrated electron density, n_e . Time evolution of impurity lines also showed a positive correlation between C IV and O VI lines. The reason of this correlation is that water on the surface of carbon tiles comes out when the plasma surface interaction occurs. Weak

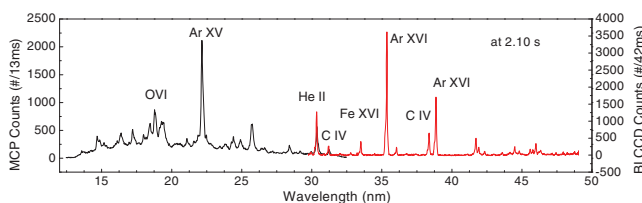


FIG. 3. VUV spectra for Ar puffing experiment at KSTAR shot #7566. Ar-gon gas was puffed at 2.0 s for 20 ms.

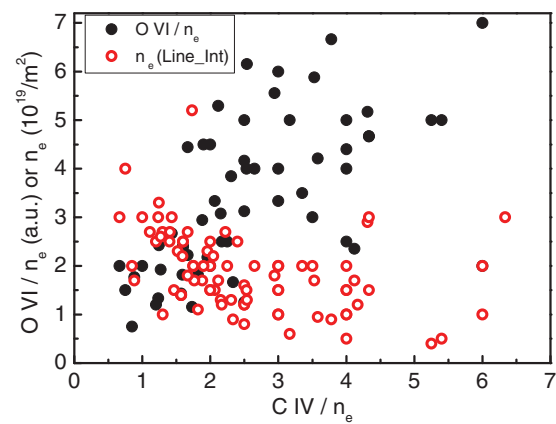


FIG. 4. Correlation between C IV vs. O VI emission intensities (closed circle), and correlation between C IV emission intensities vs. line integrated electron densities (open circle).

correlation between C IV and Fe XVI was also found because the stainless steel is the structural material of KSTAR. For plasma parameters, correlation between C IV/ n_e emission intensity and n_e was also found as shown in Fig. 4. Weak positive correlation between C IV/ n_e and the electron temperature could be found.

V. CONCLUSION

In this work, the two-channel prototype ITER VUV spectrometer was developed and each spectrometer was absolutely calibrated. To verify the calibration method for ITER VUV system, the calibration points from the hollow cathode lamp were measured and the result was compared from the calculated curves. The measured calibration result was consistent with the expected calibration curves. For the application of the calibrated prototype ITER VUV spectrometer, the prototype spectrometer was installed at KSTAR. From the measurement of KSTAR plasmas in two campaign periods, strong positive correlation between the O VI and the C IV emission intensities could be found.

ACKNOWLEDGMENTS

This work has been supported by the Ministry of Science, ICT and Future Planning of the Republic of Korea under the Korean ITER project contract.

- ¹S. Morita and M. Goto, *Rev. Sci. Instrum.* **74**, 2036 (2003).
- ²W. Biel, R. Barnsley, and G. Bertschinger, *Proceedings of 31st EPS Conference*, London, ECA Vol. 28G, P.1.134, 2004.
- ³W. Biel, G. Bertschinger, and the TEXTOR Team, *Rev. Sci. Instrum.* **75**, 2471 (2004).
- ⁴C. R. Seon, S. H. Choi, M. S. Cheon, S. Pak, H. G. Lee, W. Biel, and R. Barnsley, *Rev. Sci. Instrum.* **81**, 10E508 (2010).
- ⁵W. Biel, A. Greiche, R. Burhenn, E. Jourdain, and D. Lepere, *Rev. Sci. Instrum.* **77**, 10F305 (2006).
- ⁶K. Danzmann, M. Günther, J. Fischer, M. Kock, and M. Kühne, *Appl. Opt.* **27**, 4947 (1988).
- ⁷J. Hollandt, M. Kühne, and B. Wende, *Appl. Opt.* **33**, 68 (1994).
- ⁸D. G. Simons, G. W. Fraser, P. A. J. De Korte, J. F. Pearson, and L. De Jong, *Nucl. Instrum. Methods Phys. Res., Sect. A* **261**, 579 (1987).
- ⁹L. Poletto, A. Boscolo, and G. Tondello, *Appl. Opt.* **38**, 29 (1999).
- ¹⁰H. Garnir and P.-H. Lefebvre, *Nucl. Instrum. Methods Phys. Res., Sect. B* **235**, 530 (2005).
- ¹¹A. Greiche, W. Biel, O. Marchuk, and R. Burhenn, *Rev. Sci. Instrum.* **79**, 093504 (2008).